The low-Reynolds number spreading of axisymmetric drops and gravity currents along a free surface

Chad W. Dorsey
Department of Physics, University of Oregon, Eugene, Oregon 97403

Michael Manga
Department of Geological Sciences, University of Oregon, Eugene, Oregon 97403

(Received 29 October 1997; accepted 16 July 1998)

Experimental results are presented for the spreading of buoyant drops and gravity currents along a free surface. The spreading occurs at low Reynolds number, and no interfacial tension exists between the spreading and ambient fluid. Theoretical results suggest that distinct spreading rates occur in three regimes: $\lambda \ll [\ln(R/a)]^{-1} a/R$, $a/R \ll \lambda \ll R/a$, and $\lambda \gg R/a$, where λ is the ratio of the spreading and ambient fluid viscosities and R/a is the aspect ratio of the drop or current. Experimentally measured spreading rates in these three regimes show agreement with the theoretical solutions for long-term spreading. © *1998 American Institute of Physics.* [S1070-6631(98)00811-3]

A buoyant drop rising toward a free surface spreads laterally beneath the surface, driven by buoyancy forces. A buoyant fluid disk released at a free surface will spread similarly, as a gravity current along the surface. Figure 1 illustrates these geometrical and physical parameters for a spreading drop and a disk-shaped gravity current. The fluids have viscosity μ and density ρ, with the subscripts 0, 1, and 2 referring to the ambient, spreading, and topmost fluids, respectively. Here we consider spreading for which the Reynolds number is much less than one and the fluids are miscible, the limits relevant to geophysical processes in the Earth's mantle.[1–3]

The asymptotic spreading behavior of drops and currents depends upon their aspect ratio, R/a, and the viscosity contrast $\lambda \equiv \mu_1/\mu_0$. For intermediate viscosity ratios, $a/R \ll \lambda \ll R/a$, Lister and Kerr[4] find that

$$R \sim t^{1/5}, \tag{1}$$

where t represents time. For low viscosity ratios, $\lambda \ll [\ln(R/a)]^{-1} a/R$,

$$R \sim [t \ln t]^{1/5}, \tag{2}$$

and for high viscosity ratios, $\lambda \gg R/a$,

$$R \sim t^{1/2}, \tag{3}$$

where relations (2) and (3) are derived by Koch and Koch.[5] We will refer to these three solutions as the intermediate-viscosity, low-viscosity, and high-viscosity solutions, respectively. Koch and Koch[5] refer to these as lubrication, slender-body, and stiff solutions, respectively, reflecting the approaches used to obtain Eqs. (1)–(3). A fourth spreading regime also exists, as shown by Lister and Stone for a drop in a rotating fluid.[6] Currents spend comparatively little time in this regime, however, and this limit is not considered here. In all cases, the spreading of drops and currents will approach the intermediate-viscosity solution at very long times.[5]

For experiments in the high- and low-viscosity regimes, we injected the spreading fluid with a syringe into a cylinder 3.5 cm in diameter held at the surface of the ambient fluid. By lifting the cylinder, we released the spreading fluid as an axisymmetric gravity current. For experiments in the intermediate-viscosity range, we injected a buoyant drop of spreading fluid from a syringe attached to the tank base, allowing the drop to rise and spread below the free surface. Koch and Koch[5] show that spreading rates derived for gravity currents apply equally well to spreading drops. In experiments with $\lambda = 0.099$ and $\lambda = 0.074$, we used a graduated syringe to measure the volume of injected fluid. In all other experiments, we determined the spreading-fluid volume by weighing the apparatus and fluid before and after releasing the fluid. For experiments involving spreading drops, a layer of soybean oil 0.5 cm thick covered the ambient fluid in order to protect its surface from dust and to prevent the evaporation of water from forming a tough skin on the syrup. We also scraped the ambient fluid surface before performing

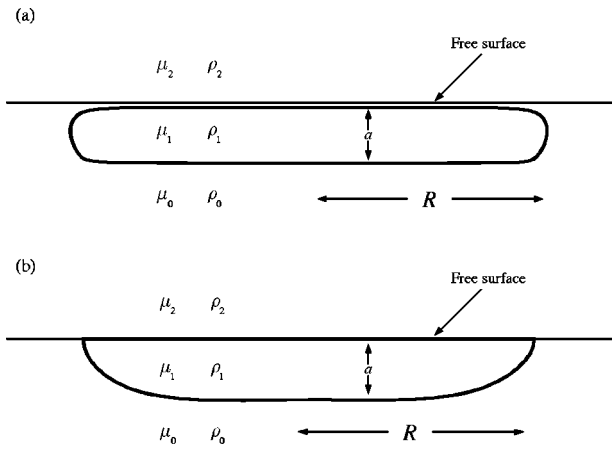

FIG. 1. (a) A drop and (b) a gravity current spreading at a free surface. Viscosities and densities are indicated by μ and ρ, respectively.

TABLE I. Experimental parameters. All specific gravities were measured with a hydrometer to an accuracy of ± 0.001 and all viscosities with a rotating viscometer to an accuracy of 2%. The fluids in each experiment are miscible.

	Intermediate-viscosity regime			High-viscosity regime	Low-viscosity regime
λ	0.099	0.074	0.24	1.0×10^{4}	4.9×10^{-4}
μ_0 (Pa s)	19.5	19.5	19.1	500	2.04
μ_1 (Pa s)	1.94	1.44	4.68	5.0×10^{-2}	1.00×10^{-3}
ρ_0 (g/cm^3)	1.412	1.412	1.419	0.918	1.366
ρ_1 (g/cm^3)	1.370	1.362	1.388	0.904	1.000
V (mL)	20	20	14.6	32.4	4.0
Ambient fluid	Corn syrup solution			Soybean oil	Corn syrup solution
Spreading fluid	Corn syrup solution			Polybutene oil	Water
Dye	Food color, chlorophenol red			None	Methyl violet 2B
Tank dimensions	Rectangular, 27×27 cm			Cylindrical, 12.7 cm radius	Cylindrical, 7.5 cm radius
Fluid depth (cm)	20	20	18	8	5

all experiments, as recommended by Lister and Kerr.[4] Table I lists spreading-fluid volumes and other relevant parameters for the experiments presented here.

For experiments in the low- and intermediate-viscosity regimes, we measured the spreading from a video image recorded by a camera positioned approximately 1 m above the free surface, thus reducing parallax errors in the measurements to ± 1 mm. A ruler or reference grid visible in the video image allowed us to convert the screen measurements to lengths. For experiments in the high-viscosity regime, we measured the current diameters directly with a ruler placed 1–2 mm above the free surface. In all experiments, we used the average of four different diameters of the currents, taken at 45° to one another, to determine the disk radius. The drops and currents remained axisymmetric during the experiments, and we did not observe any fingering instabilities.

Figure 2 shows data for three experiments in the intermediate-viscosity regime together with the asymptotic solution (1). In the experiment with $\lambda = 0.24$, the data approach and then closely follow the asymptotic solution, with $R \sim t^{0.22\pm.03}$ for times $t > 99$, where we have normalized time by the factor $\Delta\rho g R_0/\mu_0$, with R_0 representing the undeformed drop radius and $\Delta\rho \equiv \rho_0 - \rho_1$. Similar experiments by Lister and Kerr[4] in this regime were ambiguous in their agreement with Eq. (1). The data for the experiments with $\lambda = 0.099$ and $\lambda = 0.074$ also follow the predicted power-law dependence, with $R \sim t^{0.20\pm0.02}$ over the same time interval, but have proportionality constants that deviate from the predicted values. This deviation may be attributable to a gravitational instability appearing in the spreading drops.

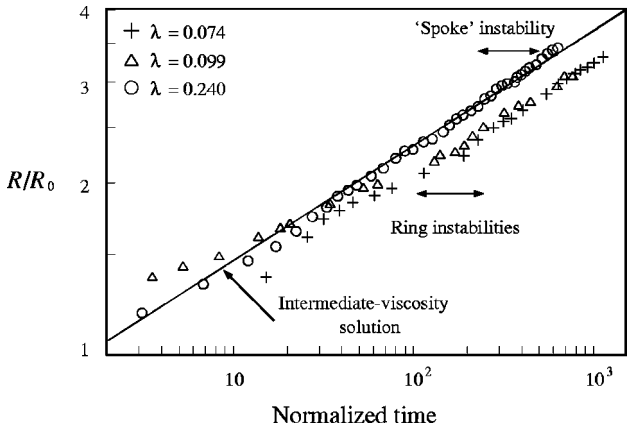

FIG. 2. Spreading in the intermediate-viscosity regime. Times are normalized by $\Delta\rho R_0 g/\mu_0$. The intermediate-viscosity solution (Ref. 5), $R = [(125V^2\Delta\rho g/256\pi\mu_0)t]^{1/5}$, where V is volume, is shown as a solid curve. Arrows indicate the times in the experiments when ring-shaped ($\lambda = 0.074$, $\lambda = 0.099$) or spoke-shaped ($\lambda = 0.24$) instabilities become well-developed.

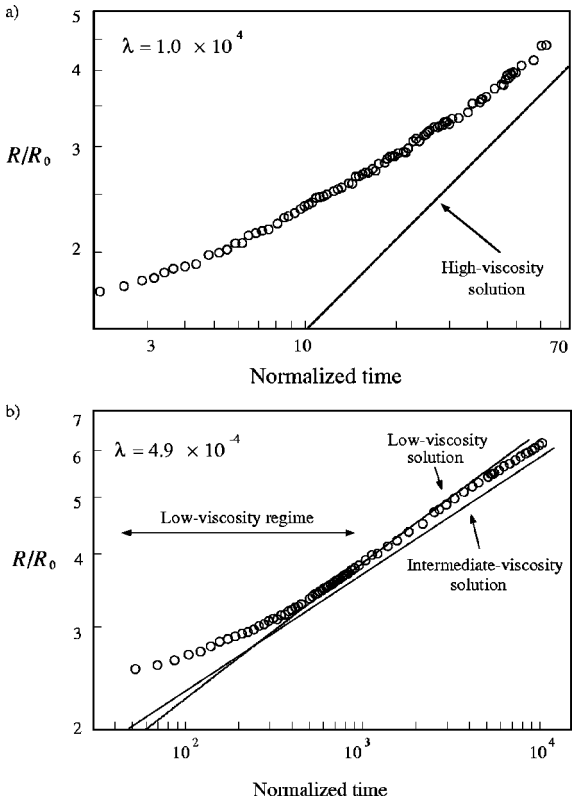

FIG. 3. (a) Spreading in the high-viscosity regime; points are experimental data and the curve is the high-viscosity spreading solution (Ref. 4), $R = [(\Delta\rho g V/6\pi\mu_1)t]^{1/2}$. Times are normalized by $\Delta\rho R_0 g/\mu_1$. (b) Spreading in the low-viscosity regime. Times are normalized by $\Delta\rho R_0 g/\mu_0$. The theoretical low-viscosity solution is obtained by integrating the velocity solution $dR/dt = (\Delta\rho g a^2/4\pi\mu_0)[\ln(4\sqrt{2}R/a) + c_1]$ numerically, where a is the current thickness and the constant $c_1 = 0.8$, as determined by Koch and Koch (Ref. 5). Arrows indicate the time interval over which the low-viscosity solution should apply.

As a drop of fluid rises toward a free surface in a denser ambient fluid, a thin layer of the ambient fluid is trapped above the rising drop. This dense layer can penetrate downward through the spreading drop as a gravitational instability. Griffiths and Campbell[1] describe instabilities that begin as an axisymmetric ring and eventually develop a more complex, irregular structure (see Fig. 8 in Ref. 1). We observed such ring-type instabilities by normalized times $t \approx 175$ in the experiments with $\lambda = 0.074$ and $\lambda = 0.099$. Some preliminary experiments in the low-viscosity regime also demonstrated axisymmetric instabilities. In the experiment with $\lambda = 0.24$, we observed an instability in the form of radially directed ''spokes'' by normalized time $t \approx 300$. Owing to experimental difficulties involved in reaching the limits of $\lambda \sim O(1)$ and greater, we were unable to determine whether viscosity contrast played a role in the type or formation of any of the observed instabilities.

Gravitational instabilities can be detected from above only once they are well-developed, and it is likely that any of the instabilities' effects on the spreading would be present earlier than these times. Noting that for times after the instabilities' development the spreading exponent for the $\lambda = 0.099$ and $\lambda = 0.074$ experiments agrees with theoretical predictions, it is plausible to assume that the fully developed instability in these experiments merely changed the effective radius and/or density of the spreading drop (both of these affect the spreading-law proportionality constant), but did not affect the power-law dependence of the spreading. In order to eliminate any possible effects of these instabilities, however, we conducted experiments in the other two viscosity regimes using gravity currents released at the free surface.

Figure 3(a) shows data taken in the high-viscosity regime together with the asymptotic solution (3). The slope of the data in the high-viscosity limit continues to increase with increasing time. With time normalized by $\Delta \rho g R_0 / \mu_1$, involving the viscosity of the spreading fluid rather than the ambient fluid, a fit to the data for $t \geqslant 50$ gives $R \sim t^{0.45 \pm 0.03}$. This slow approach of the data to the asymptotic solution is similar to the behavior of numerical solutions[5] in this viscosity limit. As in the other viscosity regimes, the spreading rate here should ultimately approach a $t^{1/5}$ behavior.

Finally, for the low-viscosity regime shown in Fig. 3(b), the spreading current reaches the low-viscosity solution at $t \approx 600$ and continues to follow the solution closely until $t \approx 1500$, where time is normalized by the factor $\Delta \rho g R_0 / \mu_0$. As it continues to spread, the current leaves the low-viscosity regime and appears to approach the intermediate-viscosity solution. Data from similar experiments performed by Griffiths and Campbell[1] should be governed by low-viscosity theory for intermediate times, and appear to undergo a similar transition at longer times, as seen in their Fig. 7(a).

ACKNOWLEDGMENTS

We are grateful to D. M. Koch and an anonymous reviewer for helpful comments and discussions. This work was supported by an NSF career grant.

[1] R. W. Griffiths and I. H. Campbell, ''Interaction of mantle plume heads with the Earth's surface and onset of small-scale convection,'' J. Geophys. Res. **96**, 18 295 (1991).
[2] R. C. Kerr and J. R. Lister, ''The spread of subducted lithospheric material along the mid-mantle boundary,'' Earth Planet. Sci. Lett. **85**, 241 (1987).
[3] D. M. Koch and M. Manga, ''Neutrally buoyant diapirs: A model for Venus coronae,'' Geophys. Res. Lett. **23**, 225 (1996).
[4] J. R. Lister and R. C. Kerr, ''The propagation of two-dimensional and axisymmetric viscous gravity currents at a fluid interface,'' J. Fluid Mech. **203**, 215 (1989).
[5] D. M. Koch and D. L. Koch, ''Numerical and theoretical solutions for a drop spreading below a free fluid surface,'' J. Fluid Mech. **287**, 251 (1995).
[6] J. R. Lister and H. A. Stone, ''Time-dependent viscous deformation of a drop in a rapidly rotating denser fluid,'' J. Fluid Mech. **317**, 275 (1996).